工學碩士

Compact Balun Filter with High Isolation by Using Phase Inverter

指導教授 姜 仁 浩

2016 年 8 月

韓國海 洋大學校 大學院

電波工學

周巖

Contents

Nomenclature

Z_0: Characteristic impedance

Z_{oe}: Even-mode characteristic impedance

Z_{oo}: Odd-mode characteristic impedance

Y_0: Characteristic admittance

Y_{oe}: Even-mode characteristic admittance

Y_{oo}: Odd-mode characteristic admittance

θ : Electrical length

ω : Angular frequency

C: Capacitance

L: Inductance

S: Scattering parameter

K: Coupling coefficient

Abstract

With the rapid development of modern network and wireless communication technology, various network equipment and electronic products can communicate through the wireless access network, all of this must depend on the critical RF module and RF components. Now days so many electronic equipments in various fields are developing toward the miniaturization, multi-function and high performance direction. In order to realize the miniaturization of wireless systems and electronic products, occupy a larger volume of RF and microwave components the need to achieve miniaturization.

In this thesis, a novel enhanced balun bandpass filter with extremely small size and high isolation is demonstrated utilizing the combination of diagonally shorted coupled lines and parallel end shorted coupled lines both with shunt lumped capacitors and parallel-strip phase inverter. The coupled lines with shunt lumped capacitors can be used to largely reduce the required electrical length of transmission line. And the parallel-strip phase inverter is utilized to realize the balanced matching and isolation. Comparing with the typical Marchand Balun, it not only has excellent performance but also has no need to add any other resistive network between the outputs.

KEYWORDS: miniaturization, coupled lines, shunt lumped capacitors, isolation balun, bandpass filter

CHAPTER 1 Introduction

Baluns are key components in many wireless and mobile communication systems as well as microwave, millimeter-wave and RF circuits such as double balanced mixers [1][2], push-pull amplifiers [3], frequency doublers [4], multipliers and antenna excitations in order to reduce the noise and higher-order harmonics and improve the dynamic range of the systems. Functionally, a balun is a device intended to act as a transformer, matching an unbalanced circuit to a balanced one,

or vice versa, with minimum loss and equal balanced impedances. The signal of a balanced circuit structure comprises two signal components with the same magnitude but 180 phase difference [5] [6].

It was desirable that the balun have a wide-band characteristic so as to make unnecessary any adjustments on the balun over a range of frequencies covered by adjusting the multifarious applications. Certain previously described wide-band transformers require a considerable amount of space because of the use of the frequency-compensating effects of one or two quarter-wave transmission line sections connected between the balun and the balanced load [7].

1.1 Background and Introduction of Balun

There are several types of baluns that are either active or passive. The major advantage of active baluns is the small size, which makes them suitable to integrate into ICs. However, the performances of active baluns including linearity, noise figure, and balance property are usually not satisfactory as well as exhaust more energy [8]. Passive baluns can be classified as lumped-type [9], coil-type [10], and distributed-type baluns [6]. The advantages of a lumped-type balun are small volume and light weight. However, it is not easy to maintain 180 phase difference and identical magnitude between the two signals.

Coil-type baluns have been widely used in lower frequency and ultra high frequency (UHF) bands. When a coil-type balun is used in higher than the UHF band, it usually has a drawback of having considerable loss. Distributed-type baluns can further be classified as a 180 hybrid balun and a Marchand balun. A 180 hybrid balun has a fairly good frequency response in the microwave frequency band. However, its size often poses a problem when it is used in the radio frequency range between 200 MHz and several GHz.

Among the various kinds of baluns, a planar version of Marchand balun, illustrated in Fig. 1.1, has been adopted for a long time due to its planar structure, good amplitude, phase balance characteristics and inherently wide operation bandwidth. Both phase difference and power distribution of a Marchand balun are reasonably good. A Marchand balun is commonly used in the industry comprises two sections of quarter-wave coupled lines [11] which may be realized using parallel-coupled microstrip lines [12], Lange couplers [13], multilayer coupled structures [14], or spiral coils [9]. Nevertheless, the Marchand balun consisting of two identical $\lambda/4$ coupled lines still occupies a big area, especially at low Frequencies.

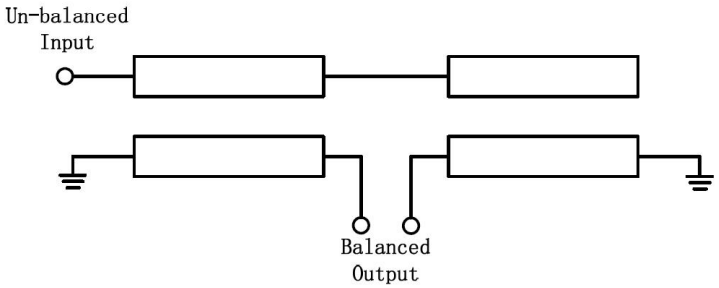

Fig. 1.1 A planar version of Marchand balun

The first transmission line balun was described in the literature by Lindenblad [15] in 1939 and variations on his original scheme soon followed. Among these was that of Marchand, who introduced a series open-circuited line to compensate for the short

circuited line reactance of the two wires. Three other variations were cataloged and described by the Harvard Radio Research Laboratory staff [16]. Harvard's Type II balun is similar to Marchand's variation but without compensation. Because of the compensating feature of Marchand's variation, the author suggests the name "compensated balun" to distinguish it from the others. In 1957, Roberts [7] apparently reinvented the compensated balun and the author used Roberts' paper as a starting point of his initial analysis [17]. In 1958, McLaughlin, Dunn, and Grow [18], using Marchand's paper, designed a 13-to-1 bandwidth

compensated balun which is the broadest thus far published. Bawer and Wolfe [19] subsequently applied the compensated balun to a broadband spiral antenna.

In design of a coupled-line Marchand balun, various analysis methods were presented. They are usually designed through circuit simulations using full-wave electromagnetic analysis [1] or lumped-element models [9]. Various synthesis techniques using coupled-line equivalent-circuit models and analytically derived scattering parameters have also been reported [20]. In [2], use of the relationships of the power wave in a balun to derive the scattering parameters can analyze a

symmetrical Marchand balun, but the exact prediction is only valid at the center frequency. In [21], inclusion of the parameter of the electrical length of the transmission line can predict broadband performances, but the approach lacks generality. Furthermore, to achieve wider bandwidth, multiconductor coupled lines to realize tight couplings were presented. Another method is the even- and odd-mode analysis method. However, it is limited to the case of a symmetrical coupled-line Marchand balun with the maximally flat responses.

In addition, most of the work on improving the planar Marchand balun has focused on achieving wide-band performance and miniaturization. The issue of balun output

matching and isolation has not been addressed. This may be attributed to the well-known fact that a lossless reciprocal three-port network such as the balun cannot achieve perfect matching at all three ports. In many applications,

however, balun output matching and isolation can enhance circuit performance. In double-balanced diode mixers, good output matching of the local oscillator (LO) and RF baluns at the diode interfaces can reduce LO power drive requirements and improve conversion loss. In push - pull amplifiers, isolation between the transistors provided by the balun outputs can enhance amplifier stability. In [22], a resistive network connected between the balun outputs is proposed to achieve balun output matching and isolation. Combining this technique with impedance transforming Marchand baluns, a class of perfectly matched impedance-transforming baluns can be realized. Whereas, this bulky resistive network consumes a large circuit area.

In some wireless applications, especially for WLAN and Bluetooth systems, the balun frequently connects a bandpass filter (BPF) with a balanced component, such as low noise amplifier (LNA), monolithic microwave integrated circuit (MMIC). Hence an integration of a BPF and a balun is necessary to reduce the cost and the size of the functional block in the systems. Recently, to meet the need, a balanced filter has been reported. However, the balanced filter, simply, uses an

integration concept of the two components using an inter-matching circuit and, hence, the resultant filter is a very complicated component.

In this thesis, a novel balun filter for size extremely miniaturization is demonstrated utilizing the combination of diagonally shorted coupled lines and parallel end shorted coupled lines. The method of adding lumped capacitors to the conventional coupled line section can largely reduce the required electrical length of coupled line while maintaining approximately the same characteristic around the

center frequency and effectively suppress the spurious passband. Furthermore, by employing an improved resistive isolation network between the two balanced ports, the perfect balanced ports matching and isolation can be achieved. Theoretical analysis and design formulas are derived. To prove the feasibility and validity of the design equation, experimental verification of such a compact balun filter working at 1GHz is presented. It is simulated by ADS and HFSS and implemented

on printed circuit board (PCB). The fabricated balun filer has a small area of 17mm ×6mm, not including the extended space for testing, a wider upper stopband and phase difference of 180 degree at the two balanced ports over the operating frequency band. The measurement results agree well with the simulation, which demonstrates that the proposed filter has great application potential. And provided high output isolation and matched.

1.2 Organization of the Thesis

The contents of the thesis are illustrated as follows:

Chapter 1 briefly introduces the background, motivation and outline of this work.

Chapter 2 describes the size-reduction method for quarter-wave transmission line by using diagonally shorted coupled lines and parallel end shorted coupled lines both with shunt lumped capacitors. Then it presents the design procedure of such a new configuration balun filter. This chapter also introduces an improved resistive network for balanced ports matching and isolation.

Chapter 3 displays the simulated results by ADS and HFSS and the experimental and measured results of fabricated balun filter.

Chapter 4 gives the conclusion of this work.

CHAPTER 2 Isolation Balun Design Theory

The conventional parallel coupled lines are useful and widely applied structures that provide the basis for many types of components, including directional couplers, power splitters and combiners, duplexers, filters, phase shifters, transformers and the aforementioned baluns. The microstrip parallel coupled filter is first proposed by Cohn in 1958 [23]. This type of filter is popular because of its planar structure, insensitivity to fabrication tolerance, wide realizable bandwidth [24] – [26], and simple synthesis procedures [27]. However, despite its advantages, the traditional parallel coupled-line filter has several shortcomings. One of the disadvantages is that it suffers from spurious responses that are generated at the multiples of operating frequency due to the unequal even- and odd-mode phase velocities of the coupled line. The stopband rejection performance is thus severely degraded. Another is the whole length of the filter is too long. Both disadvantages greatly limit the application of this type of filter. To overcome these problems, the size reduction methods are introduced in this chapter.

2.2 Ordinary Balun Design

Among the various kinds of baluns, a planar version of Marchand balun has been adopted for a long time due to its various advantages. This kind of balun has been well developed in [22]. A block diagram of the balun is shown in Fig. 2.9. It provides balanced outputs to load terminations Z2 from an unbalanced input with source impedance Z1. In general, the impedances Z1 and Z2 are different. Thus, in addition to providing balanced outputs, the balun also needs to perform impedance transformation between the source and load impedances.

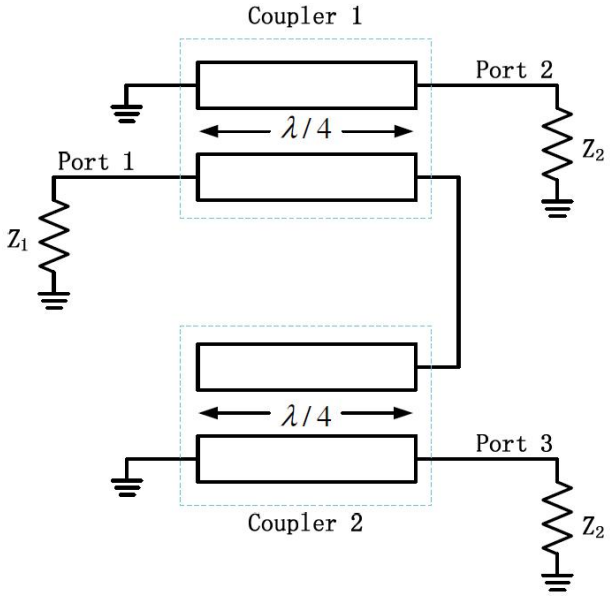

Fig.2.1 Block diagram of a symmetrical Marchand balun as two identical couplers

As shown in Fig.2.1, the planar Marchand balun consists of two coupled sections, each of which is one quarter-wavelength long at the center frequency of operation. For symmetrical baluns, the scattering matrix of the balun can be derived from the scattering matrix of two identical couplers. We just consider the case where the source and load impedances are equal to Z_1. The scattering matrix for ideal couplers with infinite directivity and coupling factor k is given by

$$[S]_{coupler} = \begin{bmatrix} 0 & k & -j\sqrt{1-k^2} & 0 \\ k & 0 & 0 & -j\sqrt{1-k^2} \\ -j\sqrt{1-k^2} & 0 & 0 & k \\ 0 & -j\sqrt{1-k^2} & k & 0 \end{bmatrix} \quad (2\text{-}1\text{-}1)$$

The S-parameters of the balun can then be obtained, which has the form

$$[S]_{balun} = \begin{bmatrix} \frac{1-3k^2}{1+k^2} & j\frac{2k\sqrt{1-k^2}}{1+k^2} & -j\frac{2k\sqrt{1-k^2}}{1+k^2} \\ j\frac{2k\sqrt{1-k^2}}{1+k^2} & \frac{1-k^2}{1+k^2} & \frac{2k^2}{1+k^2} \\ -j\frac{2k\sqrt{1-k^2}}{1+k^2} & \frac{2k^2}{1+k^2} & \frac{1-k^2}{1+k^2} \end{bmatrix} \quad (2\text{-}1\text{-}2)$$

Equation (2-1-2) shows that the use of identical coupled sections results in balun outputs of equal amplitude and opposite phase, regardless of the coupling factor and port

terminations. To achieve optimum power transfer of -3 dB to each port, we require

$$\left|S_{balun,21}\right| = \left|S_{balun,31}\right| = \frac{1}{\sqrt{2}} \tag{2-1-3}$$

With (2-1-2) and (2-1-3), the required coupling factor for optimum balun performance is given by

$$k = \frac{1}{\sqrt{3}} \tag{2-1-4}$$

When (2-1-4) is satisfied, the balun S matrix with parameters given by (2-1-2) reduces to

$$[S]_{balun} = \begin{bmatrix} 0 & \frac{j}{\sqrt{2}} & \frac{-j}{\sqrt{2}} \\ \frac{j}{\sqrt{2}} & \frac{1}{2} & \frac{1}{2} \\ \frac{-j}{\sqrt{2}} & \frac{1}{2} & \frac{1}{2} \end{bmatrix} \tag{2-1-5}$$

2.2 Isolation and Matching Network of Balun Outputs

Most of the work on improving the planar balun can achieve a perfect matching at the unbalanced port, but its poor balanced port matching and isolation limits its applications. For example, an extra output impedance-transforming matching network is needed for a push-pull amplifier design if a balun is applied at the power amplifiers' output.

To achieve perfect output port matching and isolation, some form of resistive network need to be added between the output ports which are drawn in Fig.2.2, just as in the Wilkinson power divider. Y parameters will be used to derive the required resistive network. The S parameters matrix of a balun with perfect output matching and isolation has the form [22]

$$[S]_{perfect} = \begin{bmatrix} 0 & \frac{j}{\sqrt{2}} & \frac{-j}{\sqrt{2}} \\ \frac{j}{\sqrt{2}} & 0 & 0 \\ \frac{-j}{\sqrt{2}} & 0 & 0 \end{bmatrix} \quad (2\text{-}2\text{-}1)$$

Similarly, the S matrix in (2-2-1) is converted to the Y matrix

$$[Y]_{perfert} = \begin{bmatrix} 0 & \frac{-jY_1}{\sqrt{2}} & \frac{jY_1}{\sqrt{2}} \\ \frac{-jY_1}{\sqrt{2}} & \frac{Y_1}{2} & \frac{Y_1}{2} \\ \frac{jY_1}{\sqrt{2}} & \frac{Y_1}{2} & \frac{Y_1}{2} \end{bmatrix} \quad (2\text{-}2\text{-}2)$$

It can be deduced that the Y matrix of the resistive network has the form

$$[Y]_R = \frac{1}{2Z_1}\begin{bmatrix} 1 & 1 \\ 1 & 1 \end{bmatrix} \quad (2\text{-}2\text{-}3)$$

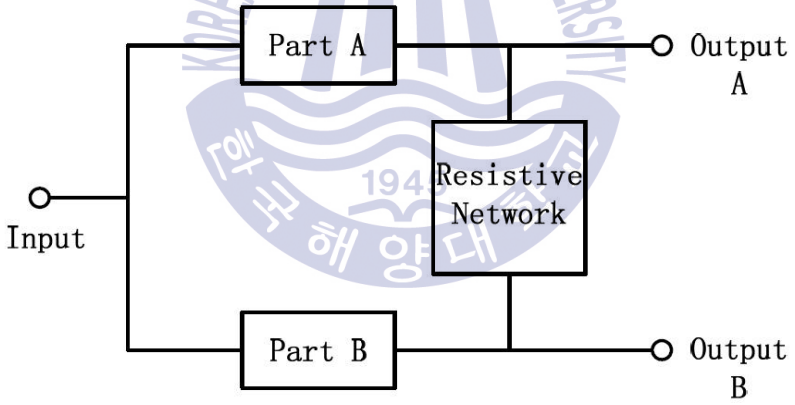

Fig. 2.2 Sketch of perfect output port matching and isolation balun with resistive network

The resistive network can be realized by a series connection of a phase inverter and a resistor of value $2Z_1$, Nevertheless, the phase inverter proposed in [22] is realized by a simple half-wavelength transmission line. This bulky resistive network consumes a large circuit area. In [28], a new technique using a physically short phase inverter network in proposed. A coupled line section grounded at each end acts as a phase inverter which takes the place the half-wavelength transmission

line. Albeit it can save the circuit proportion partly, as the electrical length of the coupled

lines is reduced, Z_{oo} becomes too small to achieve in a physical structure by the technique until now. For example, if the electrical length of the couple line is chosen as 15 degree, the odd mode characteristic impedance Z_{oo} is just 3Ohm. It means the slot of the coupled lines is unimaginable small if realize it on PCB. Whereas, the resistive network could achieve the miniaturization easily through replacing the half-wavelength transmission line in [22] by diagonally shorted coupled lines with shunted lumped capacitors as the phase inverter.

But the circuit of the network is a little huge. In order to make the circuit more compact,we used the DSPSL(the double-sided parallel-strip line) phase inverter presented by Q.Xue[31] to take place the ordinary phase inverter. And it will be introduced in next two part.

2.3 Size Reduction Method

The quarter-wavelength transmission line has been playing a very important role in many microwave circuits, functioning as impedance transformers, phase inverters and so on. However, in many cases, it is too large to be compatible with other parts of microwave systems. The size reduction method proposing by Hirota [30] is attractive in view of using short transmission line and lumped capacitors.

2.3.1 Diagonally Shorted Coupled Lines with Lumped Capacitors

The reduced quarter-wavelength transmission line using combination of shorted transmission line and shunt lumped capacitors proposed by Hirota is shown in Fig.2.3. The related equations are as follows,

$$Z_A = \frac{Z_0}{\sin\theta_A} \tag{2-3-1}$$

$$\omega C_{A1} = \frac{\cos\theta_A}{Z_0} \tag{2-3-2}$$

where Z_A, Z_0, θ_A and ω are the characteristic impedance of the shorted transmission line, the characteristic impedance of the quarter-wavelength line, the electrical length of the shorted line and angular frequency, respectively.

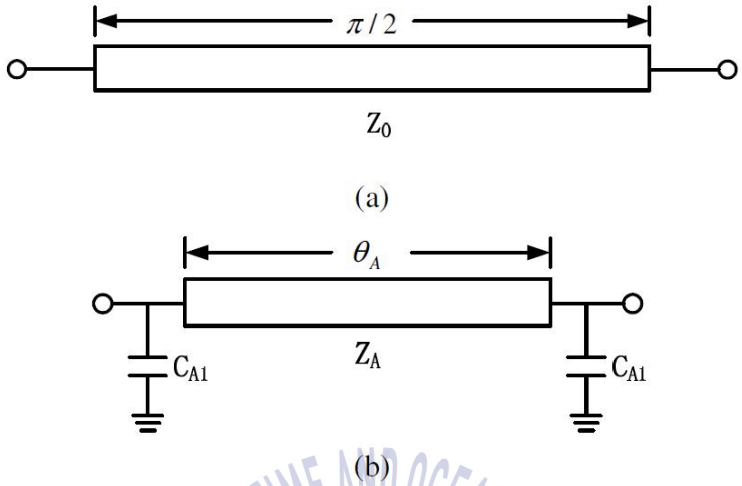

Fig.2.3 Quarter-wave transmission line (a) and its equivalent shorted transmission line circuit (b)

From (2-3-1), it is clear that the characteristic impedance of the shorted transmission line Z_A goes higher as the electrical length θ goes smaller. When it is highly miniaturized, the impedance Z_A will too high to obtain. In order to reach very small electrical length up to several degrees, the coupled line component was adopted.

Fig.2.4 (a) and (b) show the diagonally shorted coupled lines and its equivalent circuit [29].

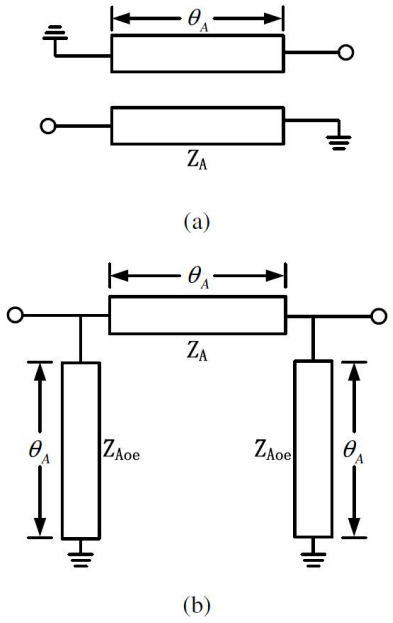

Fig.2.2 Diagonally shorted coupled lines (a) and its equivalent circuit (b)

The characteristic impedance of the diagonally shorted coupled lines can be represented by the even-mode and odd-mode characteristic impedance and thus is given by:

$$Z_A = \frac{2Z_{Aoe}Z_{Aoo}}{Z_{Aoe} - Z_{Aoo}} \tag{2-3-3}$$

In Fig.2.5, the artificial resonance circuits are inserted to Hirota's lumped distributed transmission line. Compare the dotted box part in Fig.2.5 and the equivalent circuit of the coupled lines in Fig.2.4 (b). If the following equation is satisfied, the dotted box part in Fig.2.5 can be replaced by the coupled lines [31].

$$\omega C_{A0} = \frac{1}{\omega L_{A0}} = \frac{1}{Z_{Aoe}\tan\theta_A} \tag{2-3-4}$$

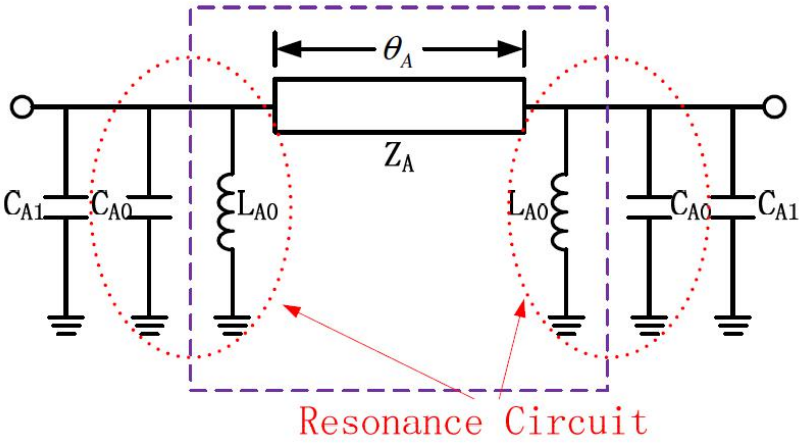

Fig.2.5 Equivalent circuit of Hirota's reduced-size transmission line including artificial resonance circuits

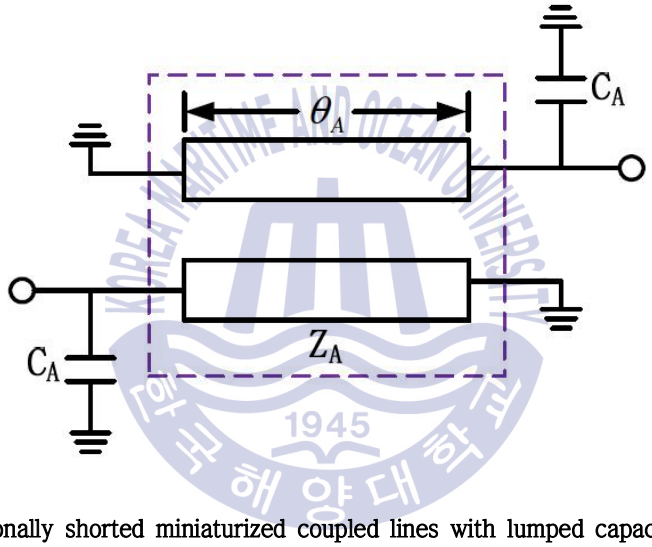

Fig.2.6 Final diagonally shorted miniaturized coupled lines with lumped capacitors equivalent to quarter-wave transmission line

Finally, the two capacitors in each side of the Fig. 2.3 can combine mathematically. The structure of the diagonally miniaturized coupled lines with lumped capacitors appears as shown in Fig 2.4.

$$C_A = C_{A0} + C_{A1} = \frac{1}{\omega Z_{Aoe} \tan\theta_A} + \frac{\cos\theta_A}{\omega Z_0} \qquad (2\text{-}3\text{-}5)$$

2.3.2 Parallel End Shorted Coupled Lines with Lumped Capacitors

As is well known, the quarter-wavelength transmission line also can be made equivalent to a lumped circuit, as given in Fig. 2.5, and the value of C_{B1} is given by

$$\omega C_{B1} = \frac{1}{Z_0} \tag{2-3-6}$$

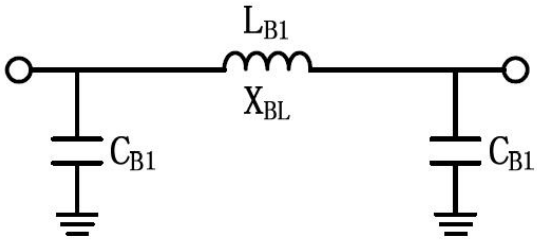

Fig.2.7 Equivalent lumped circuit of the quarter-wavelength transmission line

In order to replace the lumped inductor, firstly, the artificial resonance circuits are inserted to the circuit again at each side of the lumped inductor, as illustrated in Fig.2.8. Furthermore, the dotted network can be made equivalent to the parallel end shorted coupled line section with electrical length of θ_B in Fig.2.9 (a) and (b) when (2-3-7) and (2-3-8) are satisfied [31].

$$X_{B0} = Z_{Boe} \tan\theta_B \tag{2-3-7}$$

$$X_{BL} = \frac{2Z_{Boe}Z_{Boo}}{Z_{Boe} - Z_{Boo}} \tan\theta_B \tag{2-3-8}$$

where Z_{Boe}, Z_{Boo} are even- and odd-mode impedances of the parallel end shorted coupled line, respectively.

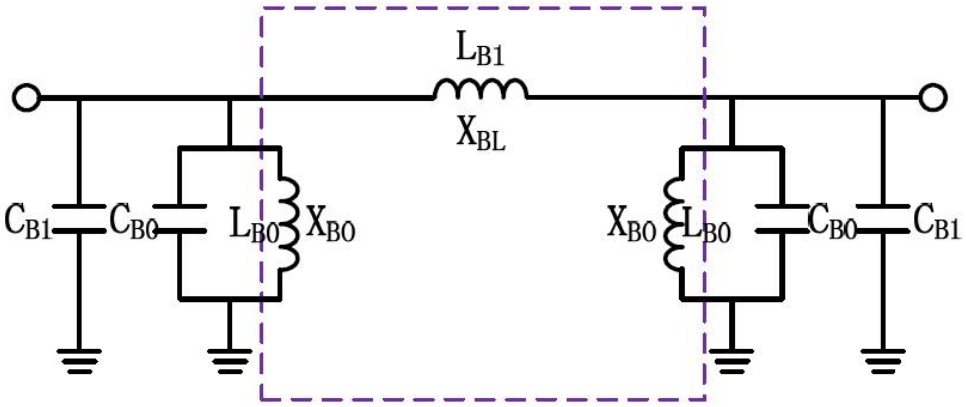

Fig.2.8 Equivalent circuit of a quarter-wavelength transmission line with artificial resonance circuits inserted

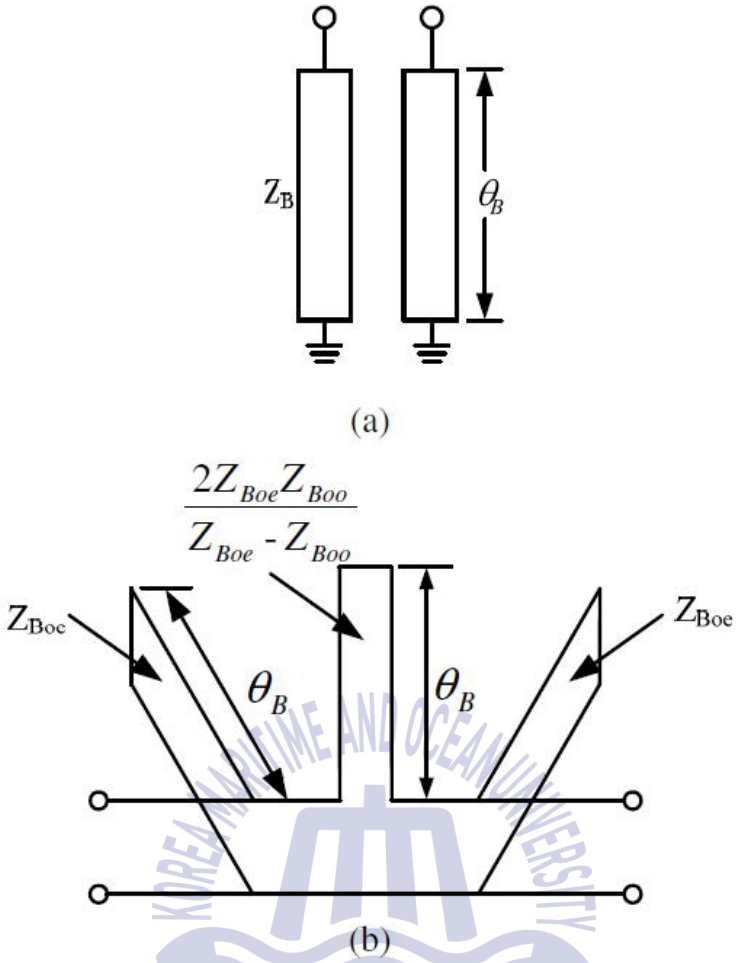

Fig.2.9 Parallel end shorted coupled lines (a) and its equivalent circuit (b)

Fig. 2.10 is the schematic diagram of the initial miniaturized bandpass filter configuration and the value of the capacitors can be deduced from (2-3-7) as:

$$\omega C_{B0} = \frac{1}{Z_{Boe} \tan\theta_B} \tag{2-3-9}$$

$$C_B = C_{B0} + C_{B1} = \frac{1}{\omega Z_{Boe} \tan\theta_B} + \frac{1}{\omega Z_0} \tag{2-3-10}$$

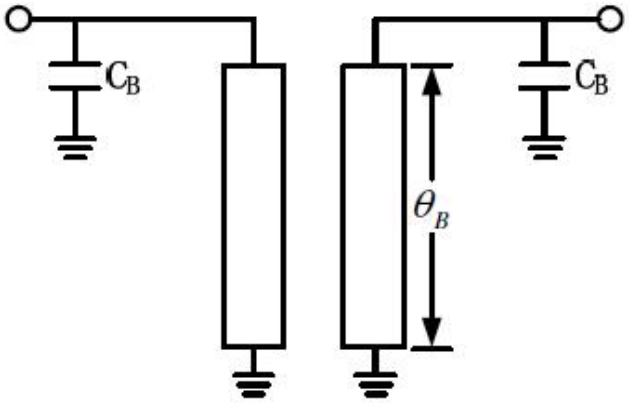

Fig.2.10 Final parallel end shorted miniaturized coupled lines with lumped capacitors equivalent to quarter-wave transmission line

With (2-3-8), if defining the relationship between the characteristic impedance of the coupled-line and its even- and odd-mode impedances, we get:

$$Z_B = \frac{2Z_{Boe}Z_{Boo}}{Z_{Boe} - Z_{Boo}} = \frac{Z_0}{\tan\theta_B} \qquad (2\text{-}3\text{-}11)$$

When the electrical length θ_B is very small for compact size, Z_B becomes very large. This large Z_B can be easily achieved by making Z_{Boe} and Z_{Boo} nearly the same.

2.4 DSPSL Phase Inverter

In this paper, we used the DSPSL phase inverter presented by Q.Xue[31].Wheeleer in 1964, the first proposed DSPSL structure, and makes a preliminary analysis using mathematical analysis method of conformal mapping thereafter Rochelle to further improve the theoretical analysis. DSPSL structure as shown in Fig.2.11, two parallel to each other the metal conduction band individually etched in the medium plate under surface.

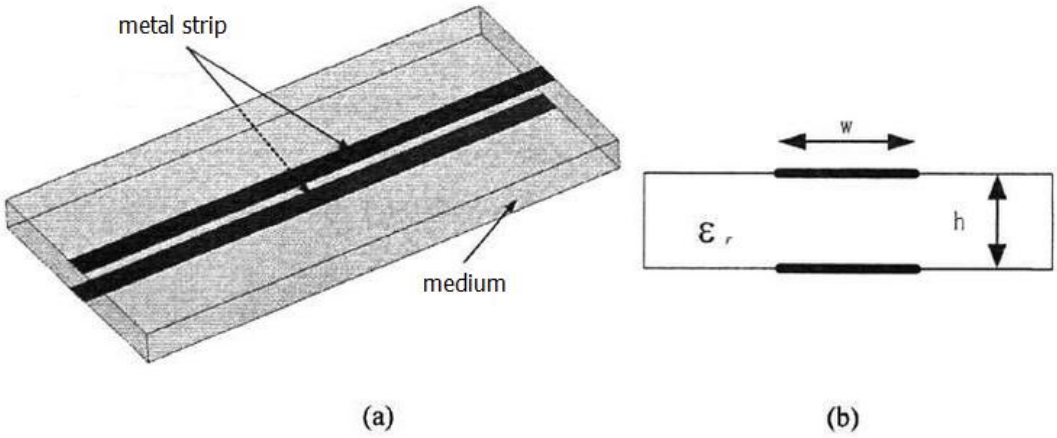

Fig.2.11 Structure of DSPSL

Microstrip line due to the small size, light weight, simple design and processing, easy and SMA connector matching links. Therefore, it has widely used. However, in this paper because of the use of the inverter of DSPSL structure and will need to transmission line transition. Transition if meet the following two conditions: 1. Transmission line electromagnetic field natural transition, 2. Good impedance matching, to achieve good performance.

The broadband transition structure between DSPSL and MSL has been reported in the literature[32]. The distribution of DSPSL is similar to that of MSL structure in the power plant, so it is easy to meet the transition conditions(Fig.2.12).

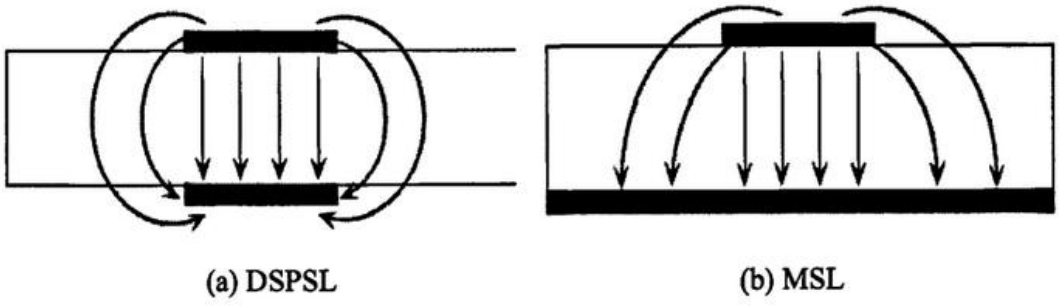

Fig.2.12 Electric field distribution diagram of cross section of DSPSL and MSL

And according to the theory of mirror image (Fig.4), the DSPSL structure can be regarded as medium in the middle of the virtual structure of two layer microstrip line connected back to back, so a thickness h of DSPSL characteristic impedance approximation

for a constant width and thickness is twice that of the microstrip line characteristic impedance of the h/2, that can be expressed as:

$$Z_1 = 2Z_2 \tag{2-4-1}$$

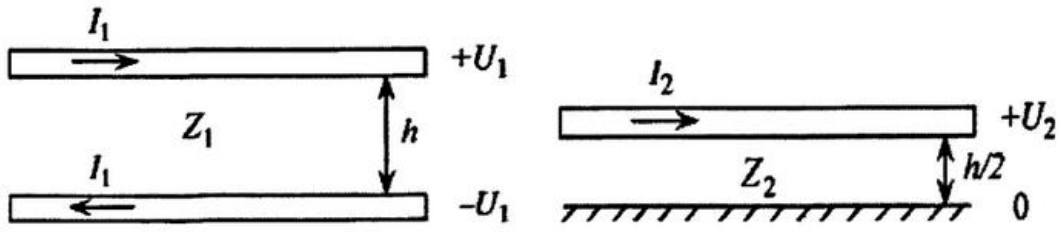

Fig.4 Mirror theory analysis of DSPSL

So we can conclude that the calculation equation of the DSPSL characteristic impedance is

$$Z = \left[\frac{174}{sqrt(\varepsilon_r + 1.41)}\right] \ln\left(\frac{2.975H}{0.8W + T}\right), 0.1 < \frac{W}{H} < 2, 1 < \varepsilon_r < 15 \tag{2-4-2}$$

Where W is the width of the DSPSL line, T is the thickness of the copper, H is the thickness of the dielectric-slab, ε r is assumed as the diclectric constant of the dielectric-slab.

Here is the DSPSL phase inverter in fig.2.14. In the figure (b) is a characteristic impedance of 50 ohm DSPSL, the figure (a) is a section with the as long as the reverse unit of the DSPSL.

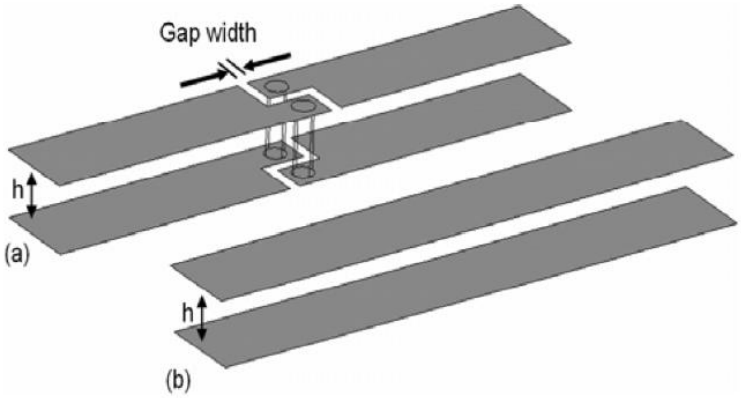

Fig.2.14 (a)DSPSL with phase inverter section (b)DSPSL

The DSPSL with the reverse unit, insertion loss in the simulation frequency range greater than -0.13dB, also at 180 degrees, in the frequency range of the simulation, the phase difference from 180 degrees to 4.2 degrees phase difference, indicating the good reversed phase performance of the structure, the most important is the characteristic and frequency independent.

2.5 New Structure for Isolation Miniaturized Balun Filter

Most of the work on improving the planar balun can achieve a perfect matching at the unbalanced port, but its poor balanced port matching and isolation limits its applications. For example, an extra output impedance-transforming matching network is needed for a push-pull amplifier design if a balun is applied at the power amplifiers' output.

First of all, because of the two kinds of miniaturized coupled lines provided in before, we can use these two section to achieve an extremely miniaturized balun filter. The corresponding Y parameters of two kinds of coupled lines expressed in terms of the even and odd mode characteristic admittances Yoe and Yoo are given in [33]

$$[Y_{couplerA}]=\begin{bmatrix} Y_{A11} & Y_{A12} \\ Y_{A21} & Y_{A22} \end{bmatrix}=\begin{bmatrix} -j\dfrac{Y_{Aoo}+Y_{Aoe}}{2}\cot\theta_A & -j\dfrac{Y_{Aoo}-Y_{Aoe}}{2}\csc\theta_A \\ -j\dfrac{Y_{Aoo}-Y_{Aoe}}{2}\csc\theta_A & -j\dfrac{Y_{Aoo}+Y_{Aoe}}{2}\cot\theta_A \end{bmatrix} \quad (2\text{-}4\text{-}3)$$

$$[Y_{couplerB}]=\begin{bmatrix} Y_{B11} & Y_{B12} \\ Y_{B21} & Y_{B22} \end{bmatrix}=\begin{bmatrix} -j\dfrac{Y_{Boo}+Y_{Boe}}{2}\cot\theta_B & j\dfrac{Y_{Boo}-Y_{Boe}}{2}\cot\theta_B \\ j\dfrac{Y_{Boo}-Y_{Boe}}{2}\cot\theta_B & -j\dfrac{Y_{Boo}+Y_{Boe}}{2}\cot\theta_B \end{bmatrix} \quad (2\text{-}4\text{-}4)$$

When there are capacitors are shunted at each side of the coupled lines, the Y parameters of two parts are

$$[Y_A]=\begin{bmatrix} Y_{A11}+j\omega C_A & Y_{A12} \\ Y_{A21} & Y_{A22}+j\omega C_A \end{bmatrix} \quad (2\text{-}4\text{-}5)$$

$$[Y_B]=\begin{bmatrix} Y_{B11}+j\omega C_B & Y_{B12} \\ Y_{B21} & Y_{B22}+j\omega C_B \end{bmatrix} \tag{2-4-6}$$

As a series of relationship about the properties of two kinds of coupled lines deduced above, every element of Y parameters in (2-4-5) and (2-4-6) can be worked out

$$\begin{aligned} Y_{A11}+j\omega C_A &= Y_{A22}+j\omega C_A = -j\frac{Y_{Aoo}+Y_{Aoe}}{2}\cot\theta_A + j(\frac{1}{Z_{Aoe}\tan\theta_A}+\frac{\cos\theta_A}{Z_0}) \\ &= j(-\frac{1}{2}Y_{Aoo}\cot\theta_A - \frac{1}{2}Y_{Aoe}\cot\theta_A + Y_{Aoe}\cot\theta_A + \frac{\cos\theta_A}{Z_0}) \\ &= j(-\frac{Y_{Aoo}-Y_{Aoe}}{2}\frac{\cos\theta_A}{\sin\theta_A}+\frac{\cos\theta_A}{Z_0}) = j(-\frac{\cos\theta_A}{Z_A\sin\theta_A}+\frac{\cos\theta_A}{Z_0}) = 0 \end{aligned} \tag{2-4-7}$$

$$Y_{A12}=Y_{A21}=-j\frac{Y_{Aoo}-Y_{Aoe}}{2}\csc\theta_A = -j\frac{Y_A}{\sin\theta_A} = -jY_0 \tag{2-4-8}$$

$$\begin{aligned} Y_{B11}+j\omega C_B &= Y_{B22}+j\omega C_B = -j\frac{Y_{Boo}+Y_{Boe}}{2}\cot\theta_B + j(\frac{1}{Z_{Boe}\tan\theta_B}+\frac{1}{Z_0}) \\ &= j(-\frac{1}{2}Y_{Boo}\cot\theta_B - \frac{1}{2}Y_{Boe}\cot\theta_B + Y_{Boe}\cot\theta_B + \frac{1}{Z_0}) \\ &= j(-\frac{Y_{Boo}-Y_{Boe}}{2}\frac{1}{\tan\theta_B}+\frac{1}{Z_0}) = j(-\frac{1}{Z_B\tan\theta_B}+\frac{1}{Z_0}) = 0 \end{aligned} \tag{2-4-9}$$

$$Y_{B12}=Y_{B21}=j\frac{Y_{Boo}-Y_{Boe}}{2}\cot\theta_B = j\frac{Y_B}{\tan\theta_B} = jY_0 \tag{2-4-10}$$

where Y_0 is the characteristic admittance of the equivalent quarter-wave transmission line of the two kinds of coupled lines. Y_1 is assumed as the characteristic admittance from the input sight. Since it is a power splitter, the relationship below is satisfied

$$Y_0=\frac{Y_1}{\sqrt{2}} \tag{2-4-11}$$

Thus, the Y parameters of the whole tri-port circuit can be derived

$$[Y]=\begin{bmatrix} Y_{A11}+Y_{B11}\omega+j\omega C_A+j\omega C_B & Y_{A12} & Y_{B12} \\ Y_{A21} & Y_{A22}+j\omega C_A & 0 \\ Y_{B21} & 0 & Y_{B22}+j\omega C_B \end{bmatrix}$$

$$=\begin{bmatrix} 0 & -jY_0 & jY_0 \\ -jY_0 & 0 & 0 \\ jY_0 & 0 & 0 \end{bmatrix}=\begin{bmatrix} 0 & \frac{-jY_1}{\sqrt{2}} & \frac{jY_1}{\sqrt{2}} \\ \frac{-jY_1}{\sqrt{2}} & 0 & 0 \\ \frac{jY_1}{\sqrt{2}} & 0 & 0 \end{bmatrix} \quad (2\text{-}4\text{-}12)$$

Based on the port terminations defined in Fig.8, (16) can be converted to the scattering parameter matrix

$$[S]=([Y_1]-[Y])([Y_1]+[Y])^{-1}$$

$$=\begin{bmatrix} Y_1-Y_{11} & -Y_{12} & -Y_{13} \\ -Y_{21} & Y_1-Y_{22} & -Y_{23} \\ -Y_{31} & -Y_{32} & Y_1-Y_{33} \end{bmatrix}\begin{bmatrix} Y_1+Y_{11} & Y_{12} & Y_{13} \\ Y_{21} & Y_1+Y_{22} & Y_{23} \\ Y_{31} & Y_{32} & Y_1+Y_{33} \end{bmatrix}^{-1}$$

$$=\frac{1}{2Y_1^3}\begin{bmatrix} Y_1 & \frac{jY_1}{\sqrt{2}} & \frac{-jY_1}{\sqrt{2}} \\ \frac{jY_1}{\sqrt{2}} & Y_1 & 0 \\ \frac{-jY_1}{\sqrt{2}} & 0 & Y_1 \end{bmatrix}\begin{bmatrix} Y_1^2 & \frac{jY_1^2}{\sqrt{2}} & \frac{-jY_1^2}{\sqrt{2}} \\ \frac{jY_1^2}{\sqrt{2}} & \frac{3Y_1^2}{2} & \frac{Y_1^2}{2} \\ \frac{-jY_1^2}{\sqrt{2}} & \frac{Y_1^2}{2} & \frac{3Y_1^2}{2} \end{bmatrix}=\begin{bmatrix} 0 & \frac{j}{\sqrt{2}} & \frac{-j}{\sqrt{2}} \\ \frac{j}{\sqrt{2}} & \frac{1}{2} & \frac{1}{2} \\ \frac{-j}{\sqrt{2}} & \frac{1}{2} & \frac{1}{2} \end{bmatrix} \quad (2\text{-}4\text{-}13)$$

To achieve perfect output port matching and isolation, some form of resistive network need to be added between the output ports which are drawn in Fig.2.16, just as in the Wilkinson power divider. Y parameters will be used to derive the required resistive network. The S parameters matrix of a balun with perfect output matching and isolation has the form [22]

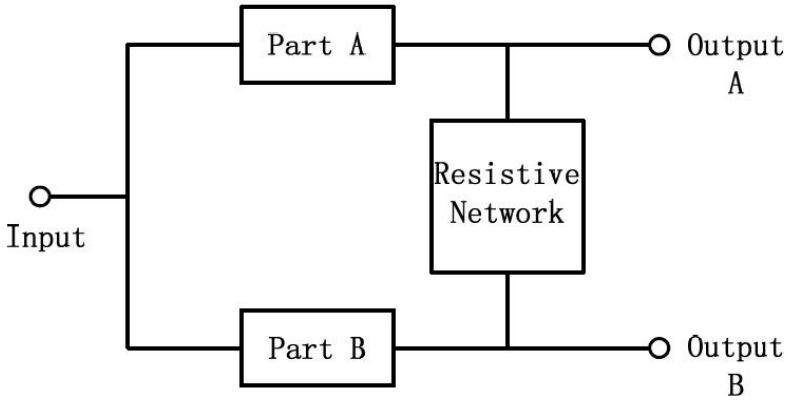

Fig.2.16 Sketch of perfect output port matching and isolation balun with resistive network

$$[S]_{perfect} = \begin{bmatrix} 0 & \frac{j}{\sqrt{2}} & \frac{-j}{\sqrt{2}} \\ \frac{j}{\sqrt{2}} & 0 & 0 \\ \frac{-j}{\sqrt{2}} & 0 & 0 \end{bmatrix} \quad (2\text{-}4\text{-}14)$$

So that we can get the Y parameters matrix from the above equation (2-4-14)

$$[Y]_{perfect} = \begin{bmatrix} 0 & \frac{-jY_1}{\sqrt{2}} & \frac{jY_1}{\sqrt{2}} \\ \frac{-jY_1}{\sqrt{2}} & \frac{Y_1}{2} & \frac{Y_1}{2} \\ \frac{jY_1}{\sqrt{2}} & \frac{Y_1}{2} & \frac{Y_1}{2} \end{bmatrix} \quad (2\text{-}4\text{-}15)$$

At the same time we can also get the ordinary balun Y parameters matrix from (2-4-13)

$$[Y]_{balun} = \begin{bmatrix} 0 & \frac{-jY_1}{\sqrt{2}} & \frac{jY_1}{\sqrt{2}} \\ \frac{-jY_1}{\sqrt{2}} & 0 & 0 \\ \frac{jY_1}{\sqrt{2}} & 0 & 0 \end{bmatrix} \quad (2\text{-}4\text{-}16)$$

From (2-4-13) and (2-4-14) we can conclude that

$$[Y]_{perfect} - [Y]_{balun} = \begin{bmatrix} 0 & 0 & 0 \\ 0 & \frac{Y_1}{2} & \frac{Y_1}{2} \\ 0 & \frac{Y_1}{2} & \frac{Y_1}{2} \end{bmatrix} \quad (2\text{-}4\text{-}17)$$

So that we conclude the below equation from above one

$$[Y_R] = \begin{bmatrix} \frac{Y_1}{2} & \frac{Y_1}{2} \\ \frac{Y_1}{2} & \frac{Y_1}{2} \end{bmatrix} = \frac{1}{2Z_1}\begin{bmatrix} 1 & 1 \\ 1 & 1 \end{bmatrix} \quad (2\text{-}4\text{-}18)$$

$[Y_R]$ is the Y parameter matrix between 2 and 3 port of the novel balun. And where Y1 is assumed as the characteristic admittance form the input sight. And then, compare the (2-4-15) and (2-4-16), there should be a network who's Y parameters matrix is (2-4-16) between output port 2 and port 3, like the Fig.2.16. $[Y_R]$ is the Y parameter matrix between 2 and 3 port of the novel balun.

Then we get the ABCD matrix in from (2-4-16)

$$\begin{bmatrix} A & B \\ C & D \end{bmatrix} = \begin{bmatrix} -1 & -\frac{2}{Y_1} \\ 0 & -1 \end{bmatrix} = -1\begin{bmatrix} 1 & \frac{2}{Y_1} \\ 0 & 1 \end{bmatrix} \quad (2\text{-}4\text{-}19)$$

In equation (2-4-17) we can see there is a -1 before the ABCD matrix, that means the resistance network is supposed to have a 180 degrees phase delay. And we also can conclude that the impedance of the resistance network value at $\frac{2}{Y_1}$, in other words is $2Z_1$. And the value Z_1 is 50Ohm.

So now we know the resistance network is supposed to have a phase inverter and series with resistor value at 100Ohm.

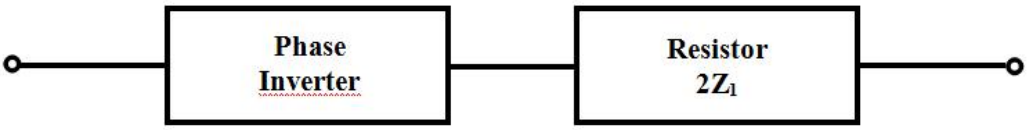

Fig.2.17 Sketch of resistive network

CHAPTER 3 Simulation, Fabrication and Measurement

From the above analysis, the coupled lines with high characteristic impedance and short electronic length are required for the miniaturized balun filter. To validate the analytical results and demonstrate the design approach, the circuit parameters are converted to physical filter structures and simulated by circuit simulation software Agilent Advanced Design System (ADS) and full-wave 3-D EM simulation tool Ansoft HFSS. For the sake of simplifying the fabrication procedure as easy as can be realized in author's laboratory room, the circuit is implemented on printed circuit board (PCB). The ideal specifications of the proposed balun filter are listed in Table 3.1.

Table 3.1 Ideal specifications of the proposed balun filter

Center frequency (GHz)	1 GHz
Fractional bandwidth (%)	16%
Insertion loss (dB)	-4.5 dB
Stopband rejection (dB)	< -60 dB up to 10 f_0
Output isolation (dB)	-22 dB

3.1 Circuit Simulating by ADS and Analysis

Although the ADS simulation and calculation are carried out in ideal cases, which have not taken many potential factors that may affect the performances of the balun into consideration. As its simulation speed is much faster than HFSS and the alteration tendency of the result can be observed easily while the circuit factors are tuning. Generally, simulation is carried out by ADS at the first step.

The initial miniaturized balun filter model illustrated in Fig.2.16 with electrical length of coupled-line being 15° was obtained. When the even-mode impedance Zoe was

arbitrarily chosen as 80 degree, the value of the lumped capacitor C_A and C_B was calculated to be 9.68 pF according to the equations (2-3-5) and (2-3-10) and the odd-mode impedance of the coupled-line Zoo was 50Ohm, making the coupling coefficient K being 0.23. The coupling coefficient K of the shorted coupled-line can determine the bandwidth of the proposed balun filter. The bandwidth increases as the coupling coefficient K does [30].

$$K = \frac{Z_{oe} - Z_{oo}}{Z_{oe} + Z_{oo}} \tag{3-1-1}$$

When the quarter-wavelength transmission line was miniaturized, one can choose a proper coupling coefficient according to the required bandwidth of the bandpass filter. However, to achieve a broad bandwidth, the coupling coefficient K should be made as large as possible, which means the difference between Zoe and Zoo should be large. It will result in a small characteristic impedance of the coupled lines and hence a large electrical length of them. Therefore, a necessary design trade-off between broad bandwidth and small circuit size should be considered.

With the obtained circuit parameters, the ADS model of the initial size-reduced balun filter was built as given in Fig. 3.1 (a) and its frequency and phase response are also shown in Fig. 3.1 (b), (c) and (d), respectively, from which we can observe the great agreement with our expectation.

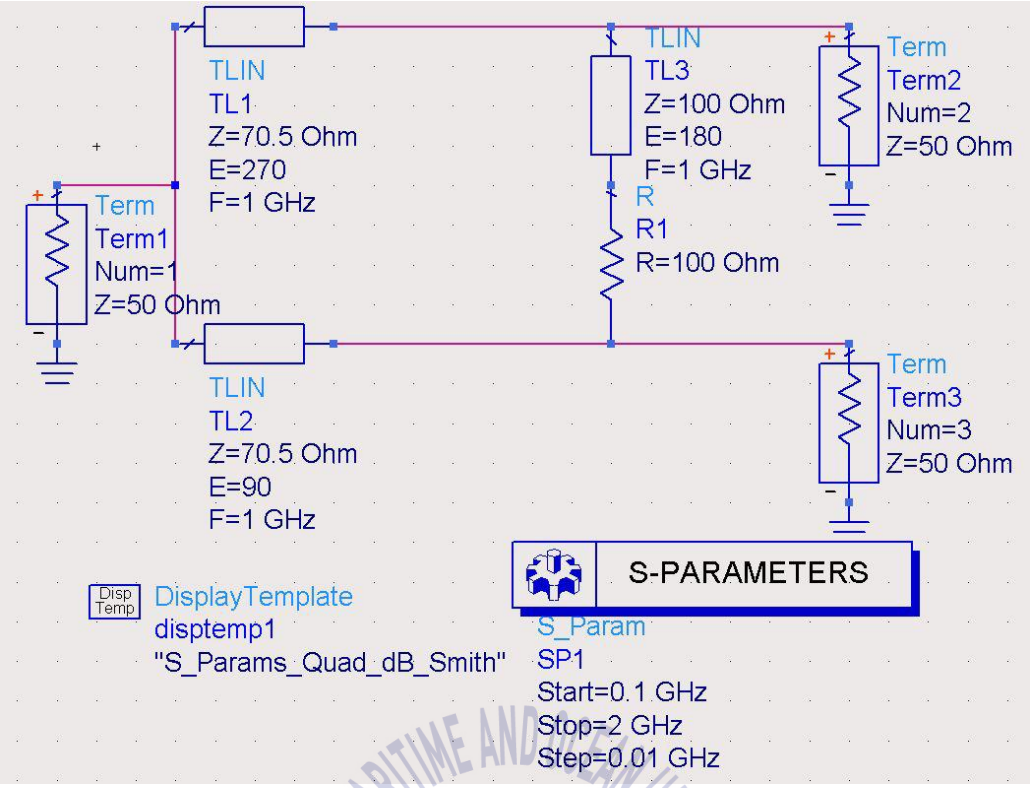

(a)

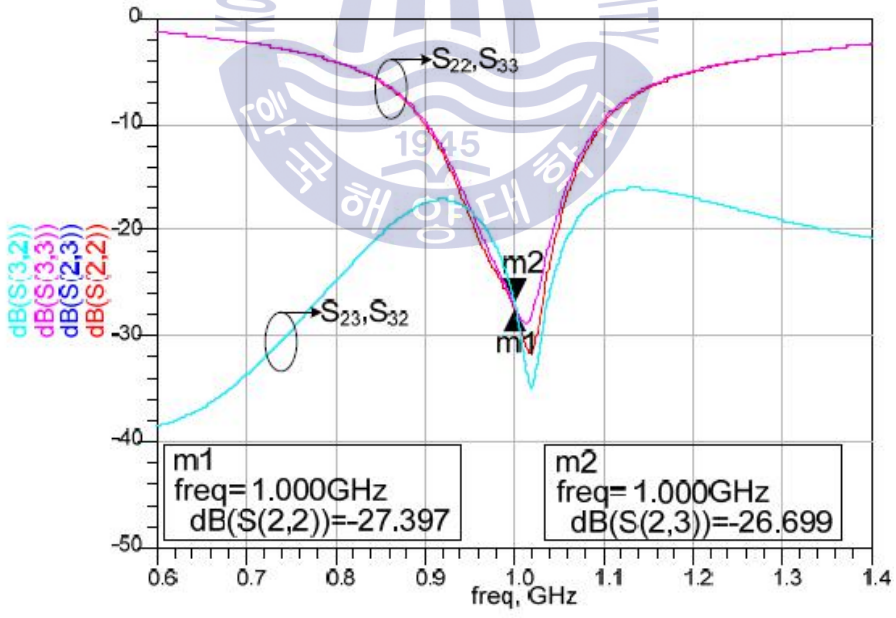

(b)

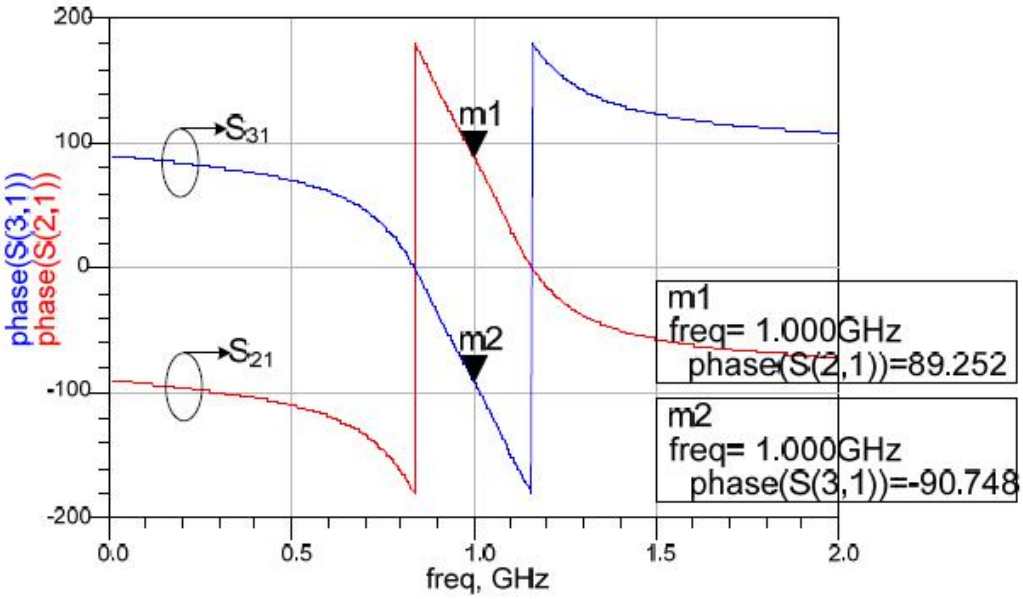

(c)

Fig. 3.1 ADS model of the perfectly matched balun with improved resistive network (a) and its frequency response of S11, S21 and S31 (b), S22, S23, S32 and S33 (c)

In many filter application, in order to reduce interference by keeping out-of-band signals from reaching a sensitive receiver, a wider upper stopband is required. However, many planar filters which are comprised of half-wavelength resonators have an inherently spurious passband at $2f_0$, where f_0 is the center frequency. In this thesis, the proposed filter is reduced to just 15 degree using combinations of two kinds of parallel coupled lines and shunt lumped capacitors. Therefore, the first spurious frequency can be shifted to much higher frequency for the electrical length of the resonant is very small.

The broadband transmission characteristic of the ADS simulation result is illustrated in Fig. 3.2. It could be noted that there is no spurious response occurs for the frequency below 10GHz. In this case, the first spurious frequency is shifted to the position which is more than 10 times of the fundamental frequency.

3.2 Full-Wave EM Simulation by HFSS and Optimization

The theoretical values calculated through the deduced equations have been confirmed through ADS simulation. And the width and length of each coupled line can be obtained by ADS Line Calculation Tool, as given in Fig.3.2.

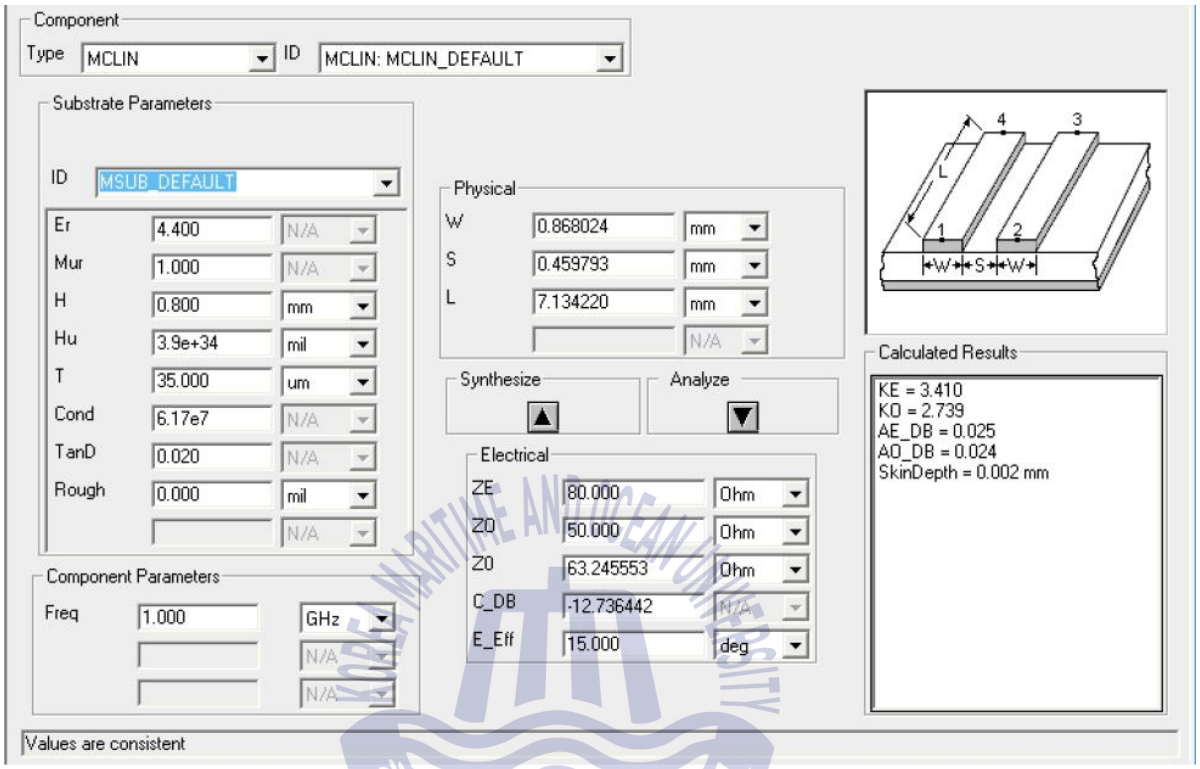

Fig.3.2 Detailed value of coupled lines calculated by ADS Linecalc

Once the bandpass filter equivalent circuit model was developed, physical filter structures such as resonators and coupled-line sections can be designed. However, one thing needs to be kept in mind: the synthesized filter model cannot be transformed into physical structures at one shot due to the parasitic components (both internally and externally). As a result, either an optimization of the filter physical dimensions or a tuning of the filter responses is necessary. Usually, it is carried out with Ansoft HFSS before fabrication until the EM simulation shows a performance close to the target one.

Table 3.2 gives the design parameters of the HFSS simulation. Fig. 3.5 (a), (b) and (c) show the layout of the balun filter drawing in HFSS and its two kinds of simulation results, respectively. Since considering the reciprocity between physical lines and optimizing the

results to an expecting one. The values of the coupled lines element have been modified slightly. We can observe that the balun filter responses simulated by the full-wave simulator are almost the same as the responses optimized by the circuit simulator ADS. This proves the validity of this design method.

Table 3.2 Design parameters of the HFSS simulation

Center frequency	1GHz
Substrate thickness	0.8mm
Substrate permittivity	4.4
Dielectric loss tangent	0.02
Copper thickness	35 μm
Copper conductivity	$6.17*10^7$
Width of coupled lines	0.65mm
Width of resistor network	1.2mm
Length of coupled lines	8.2mm
Slot of coupled lines	0.54mm
Capacitor	5.5pF
Width of transmission line	1.2mm
Ports impedance	50Ohm
Circuit size	17mm*6mm

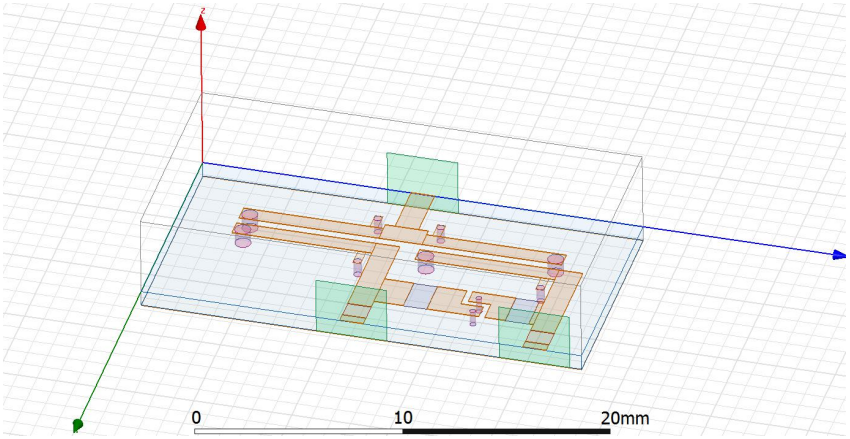

(a)

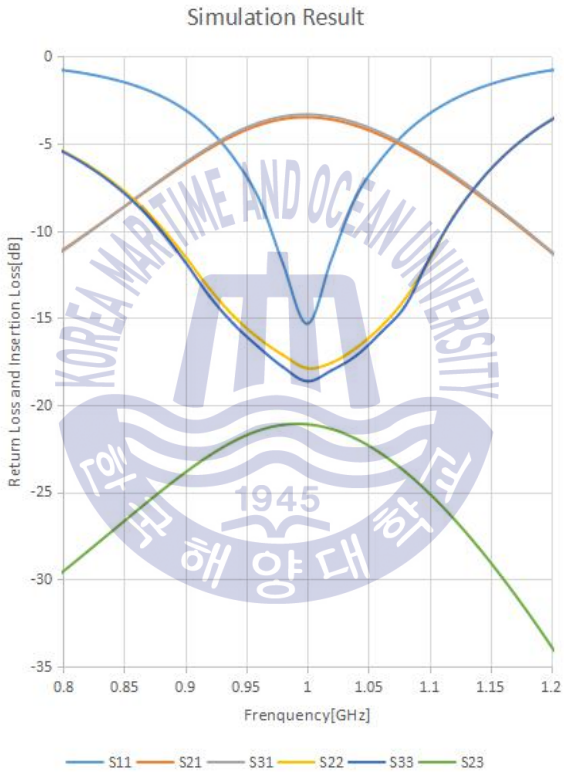

(b)

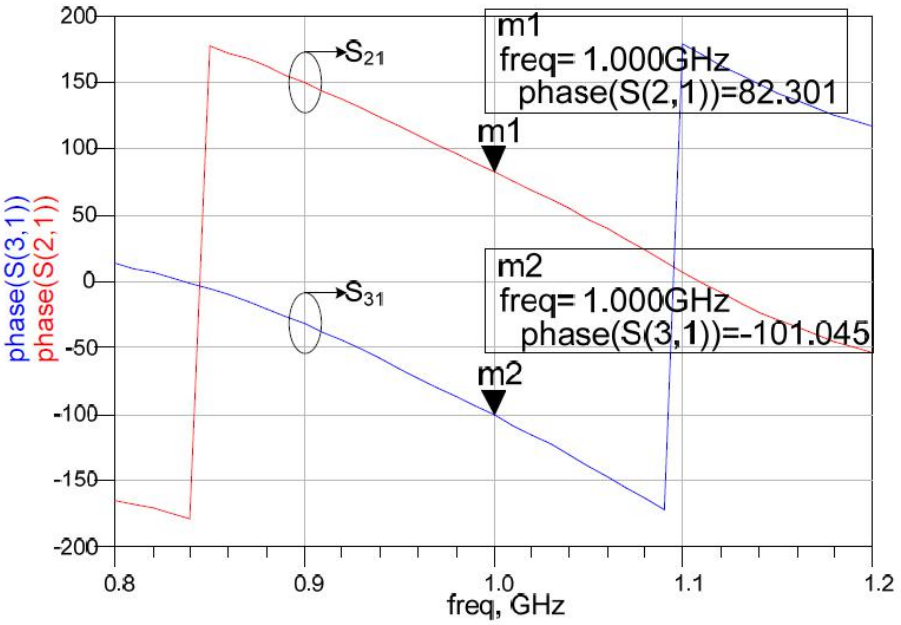

(c)

Fig.3.3 (a)Two-stage initial miniaturized balun filter model drawn in HFSS (b)HFSS simulation result of the S parameter matrix and (c) output phase difference

3.3 Fabrication and Measurement

The layout of the balun filter used in fabrication which is drawn through Auto Computer Aided Design (AutoCAD) is given in Fig.3.4, with the dimensions of the circuit area being 17mm×6mm. The balun filter is realized on the FR4 epoxy glass cloth copper-clad plat (CCL) PCB substrate having thickness 0.8mm and dielectric constant ε_r=4.4. For the measurement convenience, all the balanced and unbalanced ports impedances are assumed to be 50Ohm. The photograph of the fabricated balun is displayed in Fig. 3.6 (b).

The measured performances of the fabricated 1GHz balun filter and the comparison with HFSS simulation results are plotted in Fig. 3.7 and Fig. 3.8. The insertion loss of simulation result by HFSS is -3.22dB and measurement result is -4.2dB. It shows equal power splitting performance and good phase response. Additional loss is caused by surface

and edge roughness of the metal, inferior metal conductivity, the dielectric loss of the substrate and the inexactness of fabrication technology and so on, which were not taken into account in the calculations.

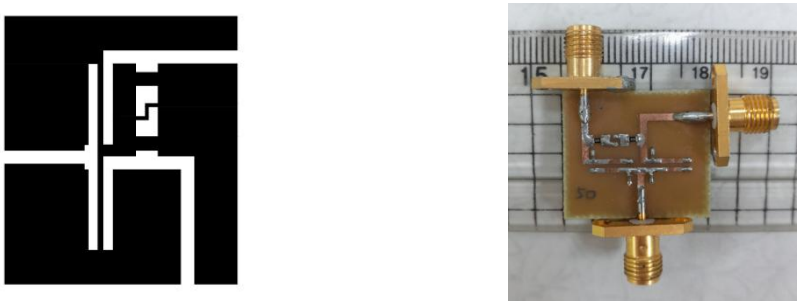

(a) (b)

Fig.3.4 layout of two-stage fabrication circuit drawn through AutoCAD (a) and its photograph (b)

In many filter application, a wider upper stopband is required. However, many planar filters which are comprised of half-wavelength resonators have an inherently spurious passband at $2f_0$, where f_0 is the center frequency. In this thesis, the proposed filter is reduced to just 15 degree. Therefore, the first spurious frequency can be shifted to much higher frequency for the electrical length of the resonant is very small.In this case, the first spurious frequency is shifted to the position which is more than 10 times of the fundamental frequency.

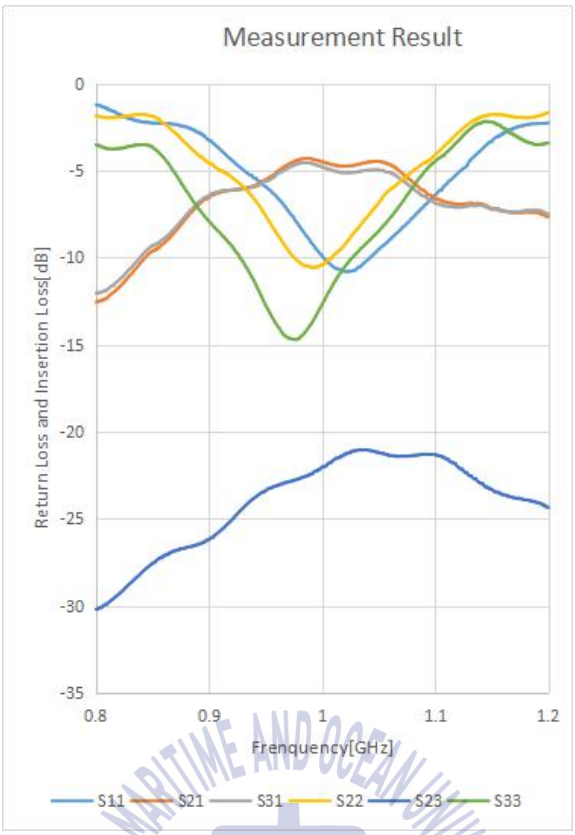

(a)

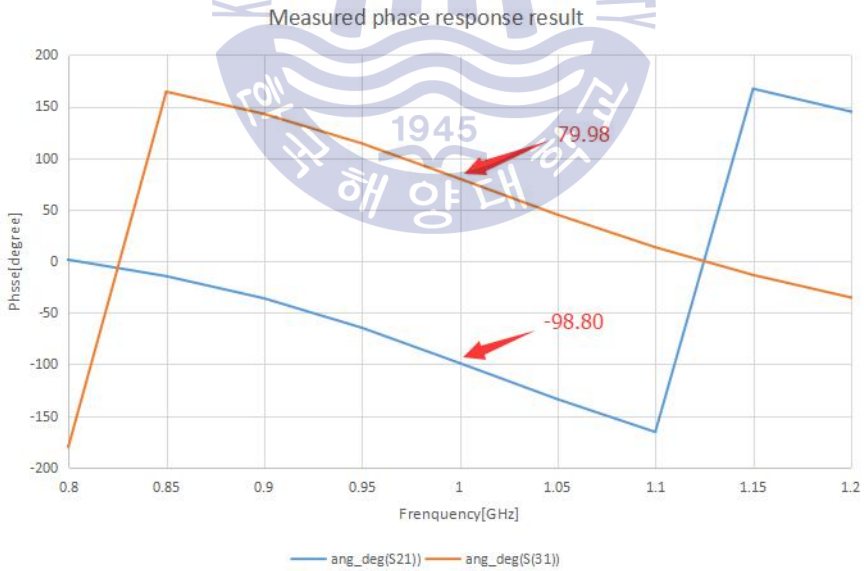

(b)

Fig.3.5 Measurement result of the S parameter matrix and output phase difference

Finally, Table3.3 summarizes the characteristic of several published isolation balun filters in comparison with this work. Obviously, the proposed bandpass filter in this paper

shows the advantage of more compact size, excellent insertion loss and high isolation characteristic, and broad bandwidth performance.

Table3.3 Comparison of different types of balun filter

Reference	This Paper	[34]	[35]		[36]	[37]
Technology	PCB	PCB	PCB	CVT	-	PCB
Center Frequency (GHz)	1	2.77	1.5	1	1.5	2
Electrical Length	$\lambda g/24$	$\lambda g/10$	$\lambda g/8$	$\lambda g/24$	$\lambda g/16.8$	$\lambda g/2$
Bandwith	$0.16f_0$	$0.09f_0$	$0.23f_0$	$0.3f_0$	$0.5f_0$	$0.1f_0$
Insertion Loss	4.5dB	5.08dB	5dB	5dB	3.2dB	3dB
Output Isolation	-22dB	-30dB	-27dB	-25dB	-24dB	-30dB
Die Area(mm^2)	17*6	23.8*28.38	15*15	20*20	-	48.97*5.12
Year	2016	2010	2010	2010	2012	2015

Chapter 4 Conclusion

In this thesis, the design theory and procedure for a novel enhanced balun bandpass filter for extremely miniaturization is carried out utilizing the combination of diagonally shorted coupled lines and parallel end shorted coupled lines both with shunt lumped capacitors which offers great amplitude and phase balance performance. A technique for achieving output matching and isolation has also been proposed. The method of adding shunt lumped capacitors to the conventional coupled line section can largely reduce the required electrical length. It shows a wider upper stopband and broad bandwidth over the operating frequency.

To demonstrate the feasibility and validity of the design equation, the size of 17mm ×6mm, not including the extended space for testing, miniaturized balun filter is designed and fabricated on PCB substrate with the thickness of 0.8mm. The electrical length of the coupled lines is reduced to 15 degree. According to the measurement results, it exhibits a bandwidth of 100MHz and 180 degree phase difference at a center frequency of 1GHz. The measurement responses agree well with simulation result curves. This class of perfectly matched baluns is invaluable in the design of balanced microwave circuits.

References

[1] Chen, Tzu-hung, et al. "Broadband monolithic passive baluns and monolithic double-balanced mixer." *Microwave Theory and Techniques, IEEE Transactions on* 39.12 (1991): 1980-1986.

[2] Tseng, Sheng-Che, et al. "Monolithic broadband Gilbert micromixer with an integrated Marchand balun using standard silicon IC process." Microwave Theory and Techniques, IEEE Transactions on 54.12 (2006): 4362-4371.

[3] Hsu, Pang-Cheng, Cam Nguyen, and Mark Kintis. "Uniplanar broad-band push-pull FET amplifiers." Microwave Theory and Techniques, IEEE Transactions on 45.12 (1997): 2150-2152.

[4] Maas, S. A., and Y. Ryu. "A broadband, planar, monolithic resistive frequency doubler." Microwave and Millimeter-Wave Monolithic Circuits Symposium, 1994. Digest of Papers., IEEE 1994. IEEE, 1994.

[5] Cho, Choonsik, and K. C. Gupta. "A new design procedure for single-layer and two-layer three-line baluns." Microwave Theory and Techniques, IEEE Transactions on 46.12 (1998): 2514-2519.

[6] K. C. Gupta and C. Cho, "A new design procedure for single-layer and two-layer three-line baluns", IEEE Trans. Microwave Theory Tech., vol. 46, no. 12, pp. 2514 - 2519, Dec. 1998.

[7] W. K. Roberts, "A new wide-band balun", Proc. IRE, vol. 4.5, pp. 1628 - 1631, Dec.1957.

[8] M. Rajashekharaiah, P. Upadhyaya and H. Deukhyoun, "A compact 5.6 GHz low noise amplifier with new on-chip gain controllable active balun", in Proc. IEEE Workshop Microelectron Electron Devices, pp. 131 - 132, 2004.

[9] Y. J. Yoon, Y. Lu, R. C. Frye, M. Y. Lau, P. R. Smith, L. Ahlquist and D. P. Kossives, "Design and characterization of multiplayer spiral transmission- line baluns", IEEE Trans. Microwave Theory Tech., vol. 47, no. 9, pp. 1841 - 1847, Sep. 1999.

[10] B. A. Munk, Balun, etc., 3rd ed, J. D. Kraus and R. J. Marhefka, Eds. New York: McGraw-Hill, ch. 23, 2002.

[11] N. Marchand, "Transmission-Line Conversion Transformers", Electronics, vol. 17, pp. 142 - 146, Dec. 1944.

[12] W. R. Brinlee, A. M. Pavio and K. R. Varian, "A novel planar double -balanced 6 - 18 GHz MMIC mixer", IEEE Microwave Millimeter-Wave Monolithic Circuit Symp. Dig., pp. 139 - 142, 1994.

[13] M. C. Tsai, "A new compact wide-band balun", IEEE Microwave and Millimeter Wave Monolithic Circuit Symp. Dig., pp. 123 - 125, 1993.

[14] K. Nishikawa, I. Toyoda and T. Tokumitsu, "Compact and broad-band three-dimensional MMIC balun". IEEE Trans. Microwave Theory Tech., vol. 47, pp. 96 - 98, Jan. 1999.

[15] N. E. Lindenblad, "Television transmitting antenna for Empire State Building ", RCA Rev., vol. 3, pp. 387-408, Apr. 1939.

[16] Radio Research Laboratory Staff, Very High-Frequency Techniques. New York: McGraw-Hill, vol. 1, p. 88, 1947.

[17] H. G. Oltman, Jr., "Analysis of the compensated balun", Rantec Corp., Calif., Tech. Rept., May 1961.

[18] J. W. McLaughlin, D. A. Dunn, and R. W. Grow, "A wide-band balun", IRE Trans. on Microwave Theory and Techniques, vol. MTT- 6, pp. 314-316, July 1958.

[19] R. Bawer and J. J. Wolfe, "A printed circuit balun for use with a spiral antenna", IRE Trans. on Microwave Theory and Techniques, vol. MTT-8, pp. 319 - 325, May 1960.

[20] R. Schwindt and C. Nguyen, "Computer-aided analysis and design of a planar multilayer Marchand balun", IEEE Trans. Microwave Theory Tech., vol. 42, pp. 1429 - 1434, July 1994.

[21] C. S. Lin, P. S. Wu, M. C. Yeh, J. S. Fu, H. Y. Chang, K. Y. Lin, and H. Wang, "Analysis of multiconductor coupled-line Marchand baluns for miniature MMIC design", IEEE Trans. Microw. Theory Tech., vol. 55, no. 6, pp. 1190 - 1199, Jun. 2007.

[22] K. S. Ang and I. D. Robertson, "Analysis and design of impedance transforming Marchand balun", IEEE Trans. Microwave Theory Tech., vol. 49, pp. 402 - 405, Feb. 2001.

[23] S. B. Cohn, "Parallel-coupled transmission-line-resonator filters", IRE Trans. Microw. Theory Tech., vol. MTT-6, no. 4, pp. 223 - 231, Apr. 1958.

[24] G. L. Matthaei, "Design of wide-band (and narrow-band) bandpass microwave filters on the insertion loss basis", IRE Trans. Microw. Theory Tech., vol. MTT-8, no. 11, pp. 580 - 593, Nov. 1960.

[25] C. Y. Chang and T. Itoh, "A modified parallel-coupled filter structure that improves the upper stopband rejection and response symmetry", IEEE Trans. Microw. Theory Tech., vol. 39, no. 2, pp. 310 - 314, Feb. 1991.

[26] A. Riddle, "High performance parallel coupled microstrip filters", in IEEE MTT-S Int. Microwave Symp. Dig., pp. 427 - 430, 1988.

[27] D. M. Pozar, Microwave Engineering, 2nd ed. New York: Wiley, pp. 474 - 485, 1998.

[28] M. Chongcheawchamnan, C. Y. Ng, K. Bandudej, A. Worapishet and I. D.Robertson, "On Miniaturization Isolation Network of an All-Ports Matched Impedance-Transforming Marchand Balun", IEEE Microwave and Wireless Components Letters, Vol. 13, No. 7, pp. 281-283, Jul. 2003.

[29] T. Hirota, "Reduced-size branch-line and rat-race hybrids for uniplanar MMIC's", IEEE Trans. Microwave Theory Tech., Vol.38, No. 3, March 1990.

[30] M. Chongcheawchamnan, C. Y. Ng, K. Bandudej, A. Worapishet and I. D. Robertson, "On Miniaturization Isolation Network of an All-Ports Matched Impedance-Transforming Marchand Balun", IEEE Microwave and Wireless Components Letters, Vol. 13, No. 7, pp. 281-283, Jul. 2003.

[31] Chiu, Leung, and Quan Xue. "Wideband parallel-strip 90 hybrid coupler with swap." *Electronics Letters* 44.11 (2008): 1.

[32] Kim, Sang-Gyu, and Kai Chang. "Ultrawide-band transitions and new microwave components using double-sided parallel-strip lines." *Microwave Theory and Techniques, IEEE Transactions on* 52.9 (2004): 2148-2152.

[33] Kang, In-Ho, and Xin Guan. "Miniaturized Microstrip Balun Filter." *Microwave Journal* 56.10 (2013).

[34] Yang, Tao, Pei-Ling Chi, and Tatsuo Itoh. "Lumped isolation circuits for improvement of matching and isolation in three-port balun band-pass filter."*Microwave Symposium Digest (MTT), 2010 IEEE MTT-S International*. IEEE, 2010.

[35] Ahn, Hee-Ran, and Tatsuo Itoh. "New isolation circuits of compact impedance-transforming 3-dB baluns for theoretically perfect isolation and matching." *Microwave Theory and Techniques, IEEE Transactions on* 58.12 (2010): 3892-3902.

[36] Montiel, Claudio M. "Folded planar Marchand balun with improved isolation for radio

frequency Automated Test Equipment applications." *Microwave Measurement Symposium (ARFTG), 2012 80th ARFTG*. IEEE, 2012.

[37] Zhang, Weiwei, et al. "Compact coupled-line balun with complex impedances transformation and high isolation." *Microwaves, Antennas & Propagation, IET* 9.14 (2015): 1587-1594.

Acknowledgement

I would like to acknowledge a number of people who have helped me during the past two years. There is no way for me to finish this thesis without their supports and encouragements.

First and foremost, my greatest appreciation surely belongs to Prof. In-Ho Kang, who guided me through the M.S. program. His creativity, broad knowledge and insight into the circuit design helped me avoid going down wrong path and shortened the path to achieve the project goal. His energy and love of what he is doing inspires me a lot. I feel very grateful for his supervision both on the technical and the personal levels during my stay in Korea.

I would also like to express my sincere gratitude to the other professors of our school for their guidance. I am particularly grateful to my thesis committee members Prof. Young Yun and Prof. Dong-Kook Park for their time and valuable suggestions in guiding and reviewing my work. My acknowledgement will not be complete without mentioning the staff members of the Department of Radio Science and Engineering for their dedication and assistance.

I want to thank all the past and present members of the RF Circuit Lab, especially Mr. Kai Wang and Mr. Xu-Guang Wang, for their professional and personal supports. There is also my gratitude to all other friends at Korea Maritime and Ocean University for the friendly environment and emotional supports. I will not forget the time we spent together before and in the future.

Additionally, I am deeply indebted to Prof. Ying-Ji Piao at Qingdao University. Without her recommendation, it is impossible for me to get this great opportunity to study in Korea.

Finally, I would like to dedicate this thesis to my family for their continued love and strong supports throughout all these years. You are always the persons who believe in and encourage me in all my endeavors, which is a contributing factor to any success I may achieve. Without these endless and priceless loves, it will never be possible for me to still live happily and accomplish my tasks. I feel great fortune to have you all accompany with me, only in this way, my life is complete and honorable.